

Crack Propagation in Double-Base Propellants

S.W. Beckwith* and D.T. Wang†
Hercules Incorporated, Magna, Utah

Crack propagation tests were conducted on a composite modified double-base (CMDB) propellant with the use of center-cracked strip biaxial specimens. Constant strain rate tests were conducted at several temperatures (40–105°F) and crosshead rates (0.02–200 in./min) to define the crack initiation and propagation characteristics for monotonically increasing strain history. The tests were conducted at ambient, 250, and 500 psig pressure to evaluate the effect of pressure on initiation and crack velocity. A second series of tests was conducted to evaluate the effect of a prestrain damage history on crack propagation. In the second series, the samples (without precrack) were initially prestrained to 15–25% and held for a period of time to induce material damage. After load release and sufficient recovery time, cracks were inserted in the specimens and they were then pulled to failure at a constant strain rate. Similar tests were conducted on round, notched tensile samples to define the critical stress intensity factor (K_{Ic}) and to provide a comparison between uniaxial and biaxial fracture initiation. Schapery's viscoelastic fracture theory was used to evaluate the crack velocity data under constant strain rate conditions. One important result of the study was the finding that the crack velocity depended rather strongly on imposed strain level.

I. Introduction

CRACK initiation and propagation in polymeric materials has been given considerable attention during the last 15 years, stimulated primarily by their unique viscoelastic behavior and also by the use of polymeric solid propellant rocket fuels. Filled polymers are used extensively as solid-propellant grains which must undergo a variety of environmental loading conditions, during motor storage and handling and during actual operational firing conditions, which impose pressure loads at high rates and for relatively long times. The consequence of a crack can be the failure of the rocket motor as a result of overpressurization, case burnthrough, erratic pressure-time response, or a variety of events related to structural or ballistic performance failure. The primary work over the last decade has been aimed at defining the laws which govern crack initiation, propagation, and trajectory under motorlike operational conditions to arrive at an assessment of overall crack criticality for a given rocket motor system.

A number of investigators have studied viscoelastic crack propagation in polymers and solid propellants.^{1–10} Most of the early work was done along the lines of classical elasticity using the Griffith solution for crack initiation. Bennett^{11,12} presented the first known data on solid-propellant crack initiation in a state-of-the-art composite propellant and noted that the fracture energy, Γ , was time- and temperature-dependent. Use of the data for motor applications was made on the basis of an energy balance using finite-element analysis. Correlation of the data with that from analysis using the thermodynamic power balance and the Williams' spherical flaw model was not quantitatively satisfactory.^{4,11} No attempt was made to monitor crack velocity during the tests. Only crack initiation was monitored by visual observation.

Knauss^{5–8,13} and Schapery^{14,15} have made significant contributions to the theoretical portion of the problem of

viscoelastic crack propagation. Knauss^{5,8} developed an approximate solution for a line crack problem which incorporates a failure zone length to introduce time and velocity effects. Knauss and Mueller^{5,6} applied the theory to an unfilled polyurethane polymer with encouraging results achieved for a variety of loading environments.

Using a stress intensity approach to fracture of solid-propellant grains, Francis et al.^{16,17} conducted a program on an unfilled polyurethane polymer (Solithane 113), an epoxy, and later, a PBAN composite propellant formulation. The primary contribution of their work was the discovery that superimposed pressure causes about a 30 to 40% increase in the stress intensity factor at a given crack velocity, thus requiring more energy to propagate the crack. This fact was essentially known, or assumed from superimposed pressure tensile tests, but was not directly related to actual crack propagation experimental data per se. The thermal and pressure loading data on small, two-dimensional samples of Solithane 113, obtained by a stress intensity factor approach, were encouraging.

Swanson¹⁸ was the first to apply fracture mechanics to composite modified double-base (CMDB) propellant. He performed a stress analysis of small, precracked, subscale STV motors formulated in terms of stress intensity factors. Using quasi-elastic analysis and time-dependent critical stress intensity factors, he was reasonably successful in predicting crack initiation in the STV subscale motors subjected to high-rate pressurization tests.

The problem of crack propagation in solid propellants has only been briefly mentioned in previous literature, leaving vast areas untouched. This is particularly true for the solid rocket motor grain itself, which must undergo a wide range of environments and loading conditions not heretofore studied in the laboratory either experimentally or analytically. Schapery^{14,15} has recently been working on a more generalized approach which may be able to resolve more complicated load histories representative of actual motor conditions. Schapery generalized the Barenblatt model¹⁹ for elastic fracture to linear viscoelastic conditions and then developed the governing equations for crack velocity in terms of the linear viscoelastic material properties.

Swanson²⁰ recently used the Schapery theory to evaluate published data on a PBAN composite propellant and found that there was a very good agreement between theory and experiment over a large range of variables. Swanson found a time-dependent fracture energy, Γ , for both crack initiation

Presented as Paper 78-170 at the AIAA 16th Aerospace Sciences Meeting, Huntsville, Ala., Jan. 16–18, 1978; submitted March 8, 1978; revision received Aug. 28, 1978. Copyright © American Institute of Aeronautics and Astronautics, Inc., 1978. All rights reserved.

Index categories: LV/M Propulsion and Propellant Systems; Solid and Hybrid Rocket Engines; Materials, Properties of.

*Technical Specialist and Supervisor. Member AIAA.

†Staff Scientist. Member AIAA.

and crack propagation must be assumed whereas Γ constant could be assumed for Solithane 113.

The present program was aimed at evaluating the Schapery theory when it was applied to a CMDB propellant under similar loading conditions. CMDB propellant is generally different than composite propellant as it has a granular filler material of a characteristic length of 0.05 to 0.07 in. and uses a nitrocellulose binder matrix instead of polyurethane and polybutadiene. Aside from the more standard loading environments of temperature, pressure, and rate (time), it was also of interest to compare multiaxial effects (uniaxial vs biaxial) and investigate the effects of prestraining damage on crack propagation characteristics. The latter is of interest to predict the behavior of a crack in a motor which must undergo previous loading history before actual ignition loads, a situation which is the case for most all missile systems in use today.

II. Theoretical Background

Schapery's Viscoelastic Fracture Theory

Schapery's theory of viscoelastic fracture, as well as some application to available polymeric materials, is discussed in Refs. 15 and 16. For completeness, the main highlights are reviewed in this paragraph, since the CMDB propellant data will be considered with respect to the existing theory in later paragraphs.

Schapery develops the theory for the time-dependent size and shape of cracks in linearly viscoelastic, isotropic media for mode I (tensile) opening stress conditions. The proposed model assumes that failure occurs in a small region behind the crack tip and is essentially equivalent to the Barenblatt model,¹⁹ except that no restriction is made on the constitutive properties of the material in the failure zone. Linear viscoelastic theory predicts the boundary around the crack tip to be cusp-shaped, a geometry which is based on the assumption of linear viscoelastic behavior in the surrounding material and which is demonstrated in several solid propellants. The singularity in stress at the crack tip due to the cohesive forces in the failure zone is equated to the negative of the singularity in stress at the crack tip due to external applied load, so that the resulting stress is everywhere finite. Schapery calculates the work done on the cohesive (failure) zone by the surrounding linear viscoelastic material and equates this to the fracture energy, Γ . The relationship for the crack velocity is then developed in the form

$$\Gamma = C_v (\tilde{t}_\alpha) K_I^2 / 8 \quad (1)$$

where Γ is the fracture energy required to produce one unit of new surface area; C_v is related to creep compliance of surrounding material; \tilde{t}_α is the characteristic time; and K_I is the opening mode stress intensity factor. The characteristic time, \tilde{t}_α , is related to the length of the failure zone, α , and the crack velocity, \dot{a} , by

$$t = \alpha / 3\dot{a} \quad (2)$$

where the time may be viewed as that required for the crack to traverse the failure zone at the crack tip. C_v is proportional to the uniaxial plane strain creep compliance which, for a constant value of Poisson's ratio, is given by

$$C_v(t) \approx 4(1-\nu^2)D(t) \quad (3)$$

Compliance (and modulus) data for polymeric materials may often be expressed as a power law in time. For a one- and two-term power law representation of C_v , Eq. (1) can be solved explicitly for the crack velocity as

$$\dot{a} = \left[\frac{C_I \lambda_n \pi^n}{\Gamma \sigma_m^{2n} I_1^{2n} 2^{2+n}} \right]^{1/n} K_I^{2(1+1/n)} \quad (4)$$

where $C_v \equiv C_I t^n$ and σ_m , I_1 are constants or material parameters defined by Schapery for the failure zone.

If one can assume that the fracture energy, Γ , is a constant, then the propagation law, Eq. (4), may be written in the form

$$\dot{a} = A K_I^{2(1+1/n)} = A K_I^q \quad (5)$$

where A becomes the term in brackets $[\]$ in Eq. (4) for constant value of Γ and $\sigma_m I_1$.

Swanson²⁰ discusses some of the possibilities of Eq. (5) if Γ is not constant and evaluates PBAN propellant data for a time-dependent value of Γ . However, the key result of Schapery's analysis is that crack propagation fracture energy cannot depend on higher-order derivatives of crack motion or histories of crack motion. For purposes of this paper, the functional dependence of Γ was not investigated but restricted to the general behavior already noted in the original objectives. Equation (5) says that the relationship between the stress intensity factor (K_I) and crack velocity (\dot{a}) is linear when plotted on log-log paper and has a slope proportional to the exponential (q).

Extension of Theory to Constant Strain Rate Tests

Since the data to be presented in subsequent sections were derived from constant strain rate tests, the crack growth law will be reformulated for the particular test at hand.

In the constant strain rate test, the applied stress, σ , is derived from the Boltzmann superposition integral for isothermal conditions as

$$\sigma(t) = R_e \int_0^t E_{rel}(t-\tau) d\tau \quad (6)$$

which, for the power law relaxation modulus given by

$$E_{rel}(t) \equiv E_I t^{-n} \quad (7)$$

results in

$$\sigma(t) = R_e E_I t^{1-n} / (1-n) \quad (8)$$

where R_e is the strain rate and E_I , n are the power law material constants.

It should be noted that the applied stress (σ) is the far-field stress which would be present for an infinite strip. The necessary correction factors for finite strip width will be discussed in the following paragraphs.

For a centrally cracked plate of infinite width, the stress is related to the stress intensity factor, K_I , and the half-crack length, a , by the expression

$$K_I = \sigma \sqrt{\pi a} \quad (9)$$

The crack growth may be expressed in terms of the applied stress (σ) by integrating Eq. (4), using the chain rule to change the independent variable from time to stress, and using the relationship between time and stress, Eq. (8), to get

$$a/a_0 = \left[1 - C_4 (a_0)^{1/r} (\sigma^P - \sigma_c^P) \right]^{-r} \quad (10)$$

where Eq. (9) has been used to express the stress intensity factor in terms of applied stress, and where

$$C_4 = \frac{A}{r} \left(\frac{\pi^{q/2}}{1-n} \right) \left(\frac{1-n}{R_e E_I} \right)^{1/(1-n)} \frac{1}{P} \quad (11a)$$

$$P = q + 1/(1-n) \quad (11b)$$

$$q = \text{experimental value from Eq. (5)} \quad (11c)$$

$$r = 2/(q-2) \quad (11d)$$

$$\sigma_c = \text{critical stress} \quad (11e)$$

Equations (11) hold when the fracture energy, Γ , is a constant, the assumption used to evaluate the CMDB data.

Finite Geometry Correction Factors

The determination of stress intensity factors from experimental data generated by finite-width centrally cracked strip biaxial specimens requires geometry correction factors. Isida²¹ generated correction factors for finite width and height for the strip biaxial sample subjected to several types of loading boundary conditions. The factors given in Ref. 21 were verified and extended over a wider range of variables by using the TEXGAP²² finite-element program. The values of K_I determined over the range of interest showed very good agreement with the original Isida values. TEXGAP and Isida values were usually within 1–2% of each other. A subroutine was written for eventual data reduction and consisted of the correction factors for finite width and height, allowing for crack growth and boundary displacement.

III. Experimental Program

Crack initiation and propagation tests were conducted in a series of experiments which involved both uniaxial and biaxial tensile tests. The uniaxial tests were used to generate fracture toughness (K_{Ic}) for uniaxial stress field conditions. The biaxial tests were designed to provide fracture toughness (K_{Ic}) values as a comparison, but, moreover, the tests were primarily used to furnish crack velocity data as a function of the imposed stress intensity factor (K_I) for a variety of environmental conditions.

The propellant used in the program is a CMDB formulation designated EJC. The propellant was taken from an eight-year-old Polaris second-stage motor. Typical uniaxial tensile properties are 195 psi maximum stress, 50% strain at maximum stress, and 570 psi initial modulus. The experimental program which was carried out is discussed in the following paragraphs.

Uniaxial Fracture Toughness (K_{Ic})

The sample used to generate uniaxial fracture toughness (K_{Ic}) values is shown in Fig. 1. The sample is rough-cut by saw from bulk propellant removed from a sectioned motor and subsequently machined on a lathe into the desired configuration. The crack, in the form of a circumferential notch, is inserted to a known depth with an Xacto knife mounted on the lathe fixture during the machining operation. Because of the nature of the test and specimen configuration, there is not believed to be any significant difference in K_{Ic} as a result of the artificial crack in comparison with a natural crack. Crack growth in this specimen is relatively fast and should not indicate any difference in behavior as a result. Once the samples are machined they are end-bonded to metal tab cylinders prior to testing.

The samples were pulled at crosshead rates ranging from 0.02 to 200 in./min with an Instron test machine for the lower rates and a closed-loop hydraulic machine for the higher

rates. The effect of temperature was determined over a range from 20 to 105°F. Since pressure is often a strong influence on the fracture characteristics of composite rubber-base propellants, the tests were also conducted at superimposed pressures of 0, 250, 500, and 1000 psig with a pressure chamber around the sample. Care was taken to ensure that the sample was not damaged due to handling and pretest loads during grip insertion.

Biaxial Fracture Characteristics

The crack initiation and propagation behavior in a biaxial stress field was defined through the use of centrally cracked strip-biaxial specimens as shown in Fig. 2. As with the uniaxial samples, the strip-biaxial specimens were prepared from bulk propellant by a similar procedure. The specimens were machined to the final configuration, after which the end tabs were bonded on. The end tabs provide the sample loading transition as well as the biaxial stress field due to the lateral bonding constraint. The end tabs were mounted in a special grip which prevents sample rotation during the test, a problem of considerable significance in crack propagation testing.

In this particular study, the crack length ($2a_0$) was selected as 1.5 in. This length corresponds to the width of commercial, single-edge razor blades, which were used to induce the artificial cracks in the specimens. The cracks were made in the specimens before testing after careful alignment of the cutting blade over the center of the specimen, equidistant from the edges. A transparent, plastic grid is superimposed over the crack area and taped in place near the grips to provide a reference base during the crack growth period. The crack pattern was made more distinct by placing a sheet of white paper on the back side of the tan-colored specimen to assist in the final photo analysis. Crack initiation and propagation were recorded and assessed through the use of slow-motion (low-rate tests) and high-speed (moderate- to high-rate tests) photography at frame rates up to 5000 frames per second.

The primary tests were conducted at crosshead rates ranging from 0.02 to 200 in./min with the Instron and closed-loop hydraulic test machines. The tests were run at temperatures of 40, 77, and 105°F after an equivalent dummy sample (same thickness) indicated temperature equilibration. The effect of superimposed pressure was also investigated at 77°F for pressure levels of 250 and 500 psig. The crack growth characteristics for the thermal tests were observed by mounting a Plexiglas door on the temperature chamber, while those for the pressure tests were observed through a 4-in.-thick Plexiglas window on the pressure chamber. Optical clarity in the pressure tests was particularly good, since the sample was located relatively close to the window and external lighting could be readily used. Care was taken to ensure that sample surface heating was avoided by using the lights only during the camera recording bursts and by keeping the burst periods short (10 s or less). The reference time was determined by the camera system (electronic frequency counter) or by a stopwatch located in the viewing area.

A second series of tests was conducted to evaluate the effects of prestrain material damage on crack propagation behavior. In this series, the strip-biaxial samples selected for the study were pulled to predetermined strain levels of 15 and 25% at the crosshead rate of 2 in./min and then held for 30

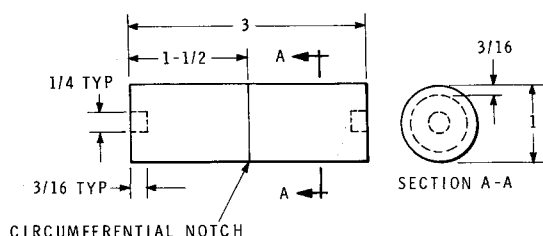


Fig. 1 Round-notched tensile sample. (All dimensions are in inches.)

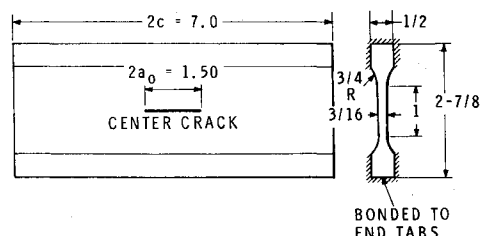


Fig. 2 Strip-biaxial sample. (All dimensions are in inches.)

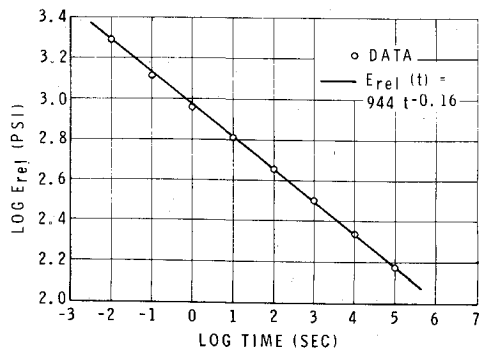


Fig. 3 Stress relaxation modulus for CMDB propellant.

min. The samples were then unloaded and allowed to relax overnight before retesting. The cracks were inserted after the recovery period and just before retesting. The tests were conducted at ambient pressure at temperatures of 40, 77, and 105°F and crosshead rates of 0.02, 2, and 200 in./min by the same procedures used for the virgin samples.

Stress relaxation modulus data, necessary for evaluation of crack growth behavior, was available from Ref. 23. These data were obtained on round end-bonded samples similar to the notched fracture toughness sample shown in Fig. 1. The strain level used for these data was typically 1/2 to 1% strain. The data are shown fitted to the power law form where E_r and n are material constants for the particular CMDB propellant. The power law fit works well over the seven decades of time shown in Fig. 3.

IV. Discussion of Results

Uniaxial and Biaxial Fracture Toughness (K_{Ic})

The critical stress intensity factor, or fracture toughness (K_{Ic}), determined from the uniaxial round-notched and strip-biaxial sample is shown in Fig. 4 as a function of the time-to-

failure, t_f . Several comments should be made concerning the method of data reduction. The value of K_{Ic} for the notched, round tensile specimen was derived from a solution by Bueckner²⁴ and given by

$$K_{Ic} = \sigma_{mn} \sqrt{\pi D} F(d/D) \quad (12)$$

where D is the outside diameter; d is the notched section diameter; σ_{mn} is the net section stress determined at maximum load; and $F(d/D)$ is the geometrical correction factor shown in Ref. 24.

The photoanalysis of the strip-biaxial samples was used to provide the value of K_{Ic} from the time at which the crack was visually observed to crack. The computer subroutine automatically input the correction factors for finite width and height. In summary, the uniaxial K_{Ic} was determined from the maximum load whereas the biaxial K_{Ic} was determined from visual observation of crack growth.

There does not appear to be any difference in behavior between uniaxial and biaxial crack initiation in the CMDB propellant. The two methods of K_{Ic} determination should not be significantly different, since the notched round tensile sample would be expected to exhibit rather fast crack growth from initiation to sample separation. Pressure also does not significantly affect the time-to-failure for the CMDB propellant. The functional form of Fig. 4 fits

$$t_f = BK_{Ic}^{-7.11} \text{ (seconds)} \quad (13)$$

where

$$B = 9.2(10^{-16})$$

Effects of Strain Rate

The evaluation of the load-time traces and the film records by using the correction factors for finite width and height results in the experimental relationship between stress in-

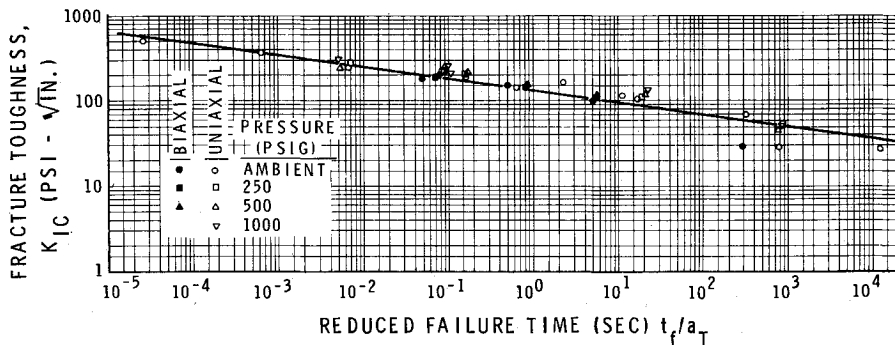


Fig. 4 Fracture toughness (K_{Ic}) for CMDB propellant.

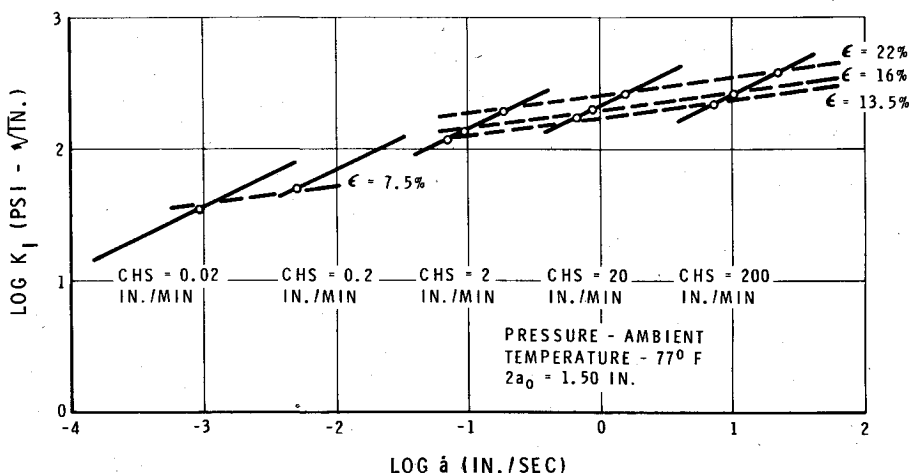


Fig. 5 Effect of strain rate on crack propagation in CMDB propellant.

tensity factors and crack velocity as shown in Fig. 5. The solid lines represent the data from four replicate tests at any one given rate and typically show less than 10% variation. Any individual curve, for a given rate, follows the form derived by Schapery in Eq. (5) with the values given by

$$\dot{a} = A_e K_I^{2.0} \quad (14)$$

where A_e depends on the particular strain rate employed. This is unusual since all previously reported data on composite propellants indicate the value of the exponent to be on the order of 6 to 7 and a continuous, smooth curve rather than a dependence on strain rate as shown. However, if one cross plots several values of K_I and \dot{a} for a fixed strain level, then it becomes readily apparent that a continuous function is found, but that the crack propagation exhibits a strong nonlinear dependence on strain level. The crack propagation law now takes on the form

$$\dot{a} = A'_{\epsilon_0} K_I^{7.50} \quad (15)$$

where the values of A'_{ϵ_0} depends on strain level. The exponent agrees reasonably well with experimental data on composite propellants as well as the value given in Eq. (13) from the crack initiation data (K_{Ic}).

There are two important aspects of Fig. 5. The first is that the data obey Schapery's power law crack propagation law, Eq. (5), over several decades of crack velocity. The second and more important aspect is that there is a strong effect of strain level on the crack propagation. This result has not been reported in the literature but is expected to be rather significant in analyzing actual rocket motor situations. Schapery²⁵ has indicated that this result is not totally unexpected on the basis of nonlinear viscoelastic behavior exhibited in composite propellants.

Closer examination of Eqs. (4) and (5) would indicate that the strain dependence could very easily enter in through the creep compliance or the description of the failure zone. Further work is needed in this area to define this dependence.

Temperature and Pressure Effects

The effects of temperature and superimposed pressure on crack propagation are shown in Figs. 6–8. The effect of temperature follows the familiar time-temperature shifting principles shown in Fig. 7. The data were shifted experimentally by using a single rate and temporarily ignoring the strain effect noted earlier. The correct procedure would entail a definition of the crack propagation law for a given

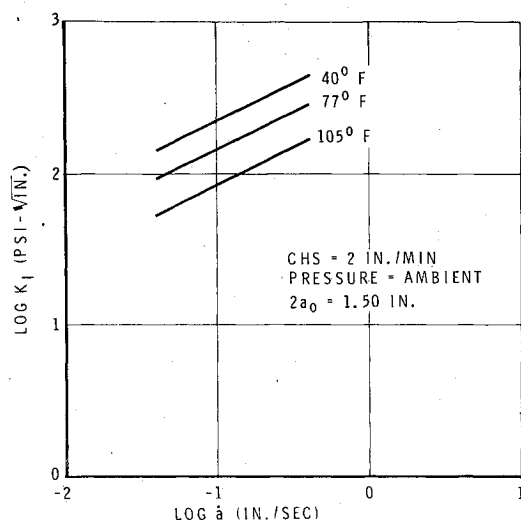


Fig. 6 Effect of temperature on crack propagation in CMDB propellant.

strain level, say 10%, followed by the shifting procedure. Pressure shows the same effect as lowering the temperature, namely, increasing the stress intensity factor at a given crack velocity. The same effects are seen in composite propellants.¹⁶ A pressure enhancement of about 25 to 30% on the stress intensity factor is realized with the addition of 500 psig.

Prestrain Damage Effects

The tests on strip-biaxial samples subjected to various levels of prestrain were conducted primarily to assess the difference in crack propagation as a result of prior load history, namely, a constant strain history to some level ϵ_0 . Figure 9 shows the result of the tests. At the highest strain rate, 200 in./min crosshead rate, no difference is seen in the crack propagation behavior after the prestrain damage cycle. Even for prestrain levels as high as 25%, no significant difference was exhibited in the response. However, as one goes to lower strain rates, possibly 0.02 in./min crosshead rate, the effect of the prestrain cycle begins to affect the crack propagation response. The effect of the prestrain is to decrease the stress intensity factor at which the crack will propagate for a fixed velocity. Referring to Fig. 5, where the effect of strain level on crack propagation was first noted, it can be seen that, at the high strain rates, the propagation takes place at a higher strain level (e.g., 14–22%). Conversely, at lower strain rates, the crack propagation begins at much lower strain levels (e.g.,

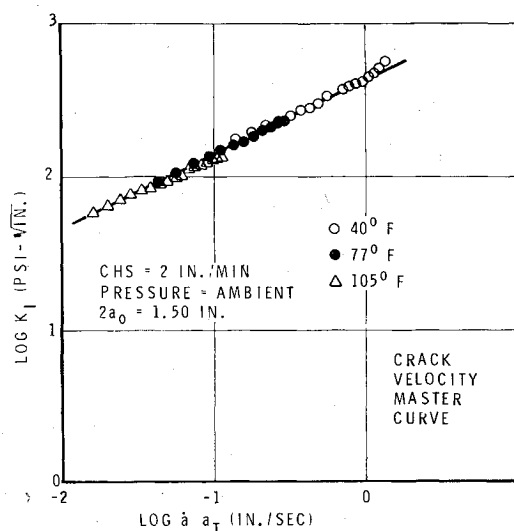


Fig. 7 Crack velocity vs. stress intensity factor master curve for CMDB propellant.

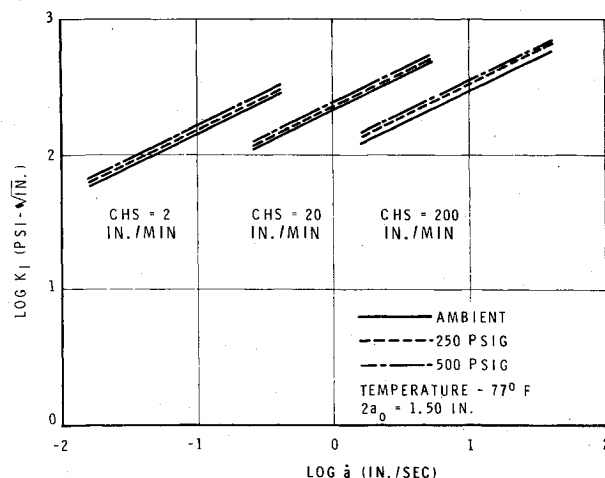


Fig. 8 Effect of pressure on crack propagation in CMDB propellant.

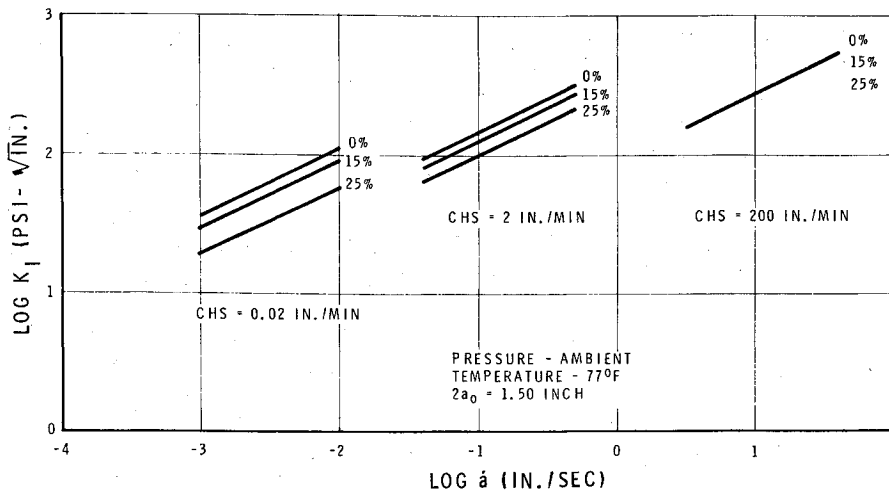


Fig. 9 Effect of prestrain damage on crack propagation in CMDB propellant.

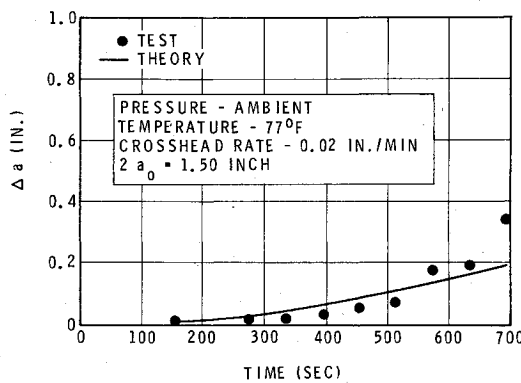


Fig. 10 Crack growth prediction for 0.02 in./min crosshead rate.

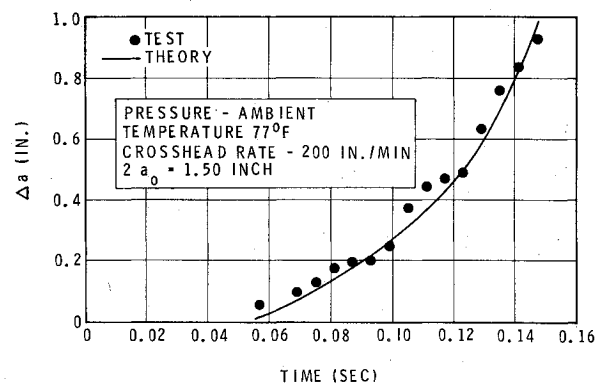


Fig. 12 Crack growth predictions for 200 in./min crosshead rate.

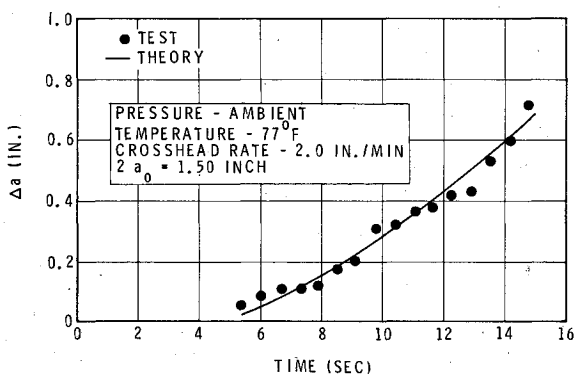


Fig. 11 Crack growth predictions for 2.0 in./min crosshead rate.

<8%). Therefore, it would not be expected to see much difference in behavior at the high strain rates for prestrain levels on the order of 15–25%. The lower strain rates should exhibit a different behavior due to the amount of microcracking which resulted from the 15–25% prestrain cycle.

Comparison with Schapery's Theory

The constant strain rate data shown in Fig. 5 was evaluated by using Schapery's theory^{14,15} to predict the crack growth from measured material properties and experimental stress values after correcting for finite geometry effects. Using Eq. (10), after reformulating to the more convenient form

$$\Delta a = a - a_0 \quad (16)$$

The data were used to predict the expected crack growth, Δa .

It should be remembered that there is some latitude in empirical fitting of the data in view of the assumptions which can be made regarding Γ . However, in viewing the data and theory as shown in Figs. 10–12, the qualitative fit of the data to the theory appears to be reasonably good, although further work is necessary in light of the strain effect.

V. Conclusions

The crack propagation behavior of CMDB propellants appear to be qualitatively similar to that previously reported for unfilled polymers (Solithane 113) and PBAN composite propellants. Both propellant systems exhibit strong temperature- and pressure-dependence on crack growth. For the CMDB propellant studied, the uniaxial and biaxial fracture toughness (K_{Ic}) are in good agreement, indicating little, if any, difference in multiaxial behavior for crack initiation for opening mode tensile conditions. Comparisons with Schapery's theory shows that the CMDB propellant obeys the power law crack propagation law, Eq. (4), and agrees qualitatively for the stress-crack growth predictions shown in Figs. 10–12.

Perhaps the most important results discussed in this paper are the strong effect of strain on crack propagation and the effect of prestrain damage cycles on low strain rate crack propagation behavior. Both of these effects are extremely important if one is to adequately characterize the material and make reliable grain predictions under thermal or pressure loading conditions.

Acknowledgments

The assistance of T.D. Pavelka in writing the computer programs for the crack propagation data analysis and of C.D. Wahlén for performing the data analysis and photographic assessment of the strip biaxial test is greatly appreciated.

References

- ¹Williams, M.L., "The Fracture of Viscoelastic Material," *Fracture of Solids*, edited by D.C. Drucker and J.J. Gilman, Interscience, New York, 1963.
- ²Bueche, F. and Halpin, J.C., "Molecular Theory for the Tensile Strength of Gum Elastomers," *Journal of Applied Physics*, Vol. 35, Jan. 1970, pp. 497-507.
- ³Rivlin, R.S. and Thomas, A.G., "Rupture of Rubber, I, Characteristic Energy for Tearing," *Journal of Polymer Science*, Vol. 10, March 1953, pp. 291-318.
- ⁴Williams, M.L., "Initiation and Growth of Viscoelastic Fracture," *International Journal of Fracture Mechanics*, Vol. 1, Dec. 1964, pp. 292-310.
- ⁵Knauss, W.G., "Delayed Failure—The Griffith Problem for Linearly Viscoelastic Materials," *International Journal of Fracture Mechanics*, Vol. 6, March 1970, pp. 7-20.
- ⁶Mueller, H.K. and Knauss, W.G., "Crack Propagation in a Linearly Viscoelastic Strip," *Journal of Applied Mechanics*, Vol. 38, June 1971, pp. 483-488.
- ⁷Knauss, W.G. and Dietmann, H., "Crack Propagation Under Variable Load Histories in Linearly Viscoelastic Solids," *International Journal of Engineering Science*, Vol. 8, Aug. 1970, pp. 643-656.
- ⁸Knauss, W.G., "Stable and Unstable Crack Growth in Viscoelastic Media," *Transactions of the Society of Rheology*, Vol. 13, 1969, pp. 291-313.
- ⁹Cheropanov, G.P., "Crack Propagation in Continuous Media," *Journal of Applied Mathematics and Mechanics (PMM)*, Vol. 31, 1967, pp. 503-512.
- ¹⁰Cheropanov, G.P., "Cracks in Solids," *International Journal of Solids and Structures*, Vol. 4, 1968, pp. 811-831.
- ¹¹Bennett, S.J., "The Use of Energy Balance in Rocket Motor Grain Integrity Studies," *JANNAF Mechanical Behavior Working Group, 8th Meeting*, CPIA Publ. 193, Vol. 1, 1970, pp. 393-403.
- ¹²Bennett, S.J., Anderson, G.P., and Williams, M.L., "The Time Dependence of Surface Energy in Cohesive Fractures," *Journal of Applied Polymer Science*, Vol. 14, March 1970, pp. 735-745.
- ¹³Knauss, W.G., "The Mechanics of Polymer Fracture," *Applied Mechanics Review*, Vol. 26, June 1973, pp. 1-17.
- ¹⁴Schapery, R.A., "A Theory of Crack Initiation and Growth in Viscoelastic Media; I—Theoretical Development," *International Journal of Fracture*, Vol. 11, Feb. 1975, pp. 141-159.
- ¹⁵Schapery, R.A., *A Theory of Crack Growth in Viscoelastic Media*, Texas A&M University, College Station, Tex., Rept. MM 2764-73-1, 1973.
- ¹⁶Francis, E.C., Carlton, C.H., and Lindsey, G.H., "Viscoelastic Fracture of Solid Propellants in Pressurization Loading Conditions," *Journal of Spacecraft and Rockets*, Vol. 11, Oct. 1974, pp. 691-696.
- ¹⁷Francis, E.C., Carlton, C.H., Deverall, L.I., Lindsey, G.H., Knauss, W.G., and Parmerter, R.R., "Application of Fracture Mechanics to Predicting Failures in Solid Propellants," AFRPL-TR-70-105, Sept. 1970.
- ¹⁸Swanson, S.R., "Crack Propagation in Double-Base Propellants Under Ignition Loading," *7th Meeting ICRPG Mechanical Behavior Working Group*, CPIA Publ. 177, 1968, pp. 131-142.
- ¹⁹Barenblatt, G.I., "The Mathematical Theory of Equilibrium Cracks in Brittle Fracture," *Advances in Applied Mechanics*, Vol. VII, Academic Press, New York, 1962, pp. 55-129.
- ²⁰Swanson, S.R., "Application of Schapery's Theory to Viscoelastic Fracture of Solid Propellant," *Journal of Spacecraft*, Vol. 13, Sept. 1976, pp. 528-533.
- ²¹Isida, M., "Effect of Width and Length on Stress Intensity Factors of Internally Cracked Plates Under Various Boundary Conditions," *International Journal of Fracture Mechanics*, Vol. 7, Sept. 1971, pp. 301-311.
- ²²Dunham, R.S. and Becker, E.R., "TEXGAP—The Texas Grain Analysis Program," University of Texas, Austin, Tex., TICOM 73-1, 1973.
- ²³DeWeese, H.B., "Polaris A-3 Second Stage Fleet Motor Analysis," Hercules Rept. R/C 2-77-93, Aug. 1973.
- ²⁴Bueckner, H.F., "Discussion of Stress Analysis of Cracks," ASTM STP 381, *Fracture Toughness Testing and Its Applications*, 1965, pp. 82-83.
- ²⁵Schapery, R.A., personal communication, Nov. 1976.